ELSEVIER
Journal of Photochemistry and Photobiology A: Chemistry 156 (2003) 243–248
Journal of Photochemistry and Photobiology A:Chemistry
www.elsevier.com/locate/jphotochem

Photocatalytic behavior of titanium oxide-perovskite type $Sr(Zr_{1-x}Y_x)O_{3-\delta}$ composite particles

Takahisa Omata, Shinya Otsuka-Yao-Matsuo*

Department of Materials Science and Processing, Graduate School of Engineering, Osaka University,
2-1 Yamada-oka, Suita, Osaka 565-0871, Japan

Received 9 July 2002; received in revised form 24 September 2002; accepted 17 October 2002

Abstract

Photocatalytic reactions sensitized by composite particles have been examined, which are composed of titanium dioxide and acceptor-doped perovskite involving alkali-earth elements. Although the photocatalytic activity of perovskite-type oxide $Sr(Zr_{0.90}Y_{0.10})O_{3-\delta}$ being p-type conductor is weak, it absorbs light with wavelength of $\lambda < 800$ nm. Titanium dioxide (TiO_2) being n-type conductor exhibits a fairly high photocatalytic activity; however, it does not absorb visible light. Under the irradiation of Xe discharge light, the composite particles involving the pn-junction exerted several times higher photocatalytic activity in photodegradation of methylene blue than a sole TiO_2. Similar results were obtained for the composite powders of $Sr(Zr_{0.95}Y_{0.05})O_{3-\delta}$, $Ca(Zr_{0.95}Y_{0.10})O_{3-\delta}$ and $Ca(Zr_{0.95}Ga_{0.05})O_{3-\delta}$ with TiO_2, respectively. Under the irradiation of visible light with wavelength of $\lambda > 420$ nm, it was found that the photodegradation of methylene blue and HCOOH aqueous solutions proceeded. These results may be explained by a model for the flow of the photogenerated electrons and holes through the pn-junctions in the composite particles.

Keywords: Photocatalysts; Composite particle; Photodegradation; Methylene blue; Formic acid; Visible light irradiation

1. Introduction

Since photo-assisted water splitting into hydrogen and oxygen on titanium dioxide (TiO_2) electrode was discovered [1,2], photocatalytic reaction sensitized by TiO_2 [3] and other semiconductor materials [4,5] has attracted extensive interest as a potential way to solve the energy and environmental issues. Most of the investigations have focused on anatase-type TiO_2 [3], because it exerts relatively high photocatalytic activity under the light irradiation with wavelength of $\lambda < 390$ nm and high chemical stability. To induce the photocatalytic reactions efficiently, it is of great importance to restrain the recombination of the photogenerated electrons and holes. To separate the photogenerated charges spatially, a well-known approach is to load co-catalysts [5], e.g. NiO, Pt, and RuO_2, on TiO_2. Another approach is to use composite films and powders consisting of two semiconducting photocatalysts, e.g. TiO_2/GaP [6], TiO_2/Nb_2O_5 [7], TiO_2/SnO_2 [8,9] and TiO_2/WO_3 [10–12].

Accepter-doped perovskite-type oxides involving alkali-earth elements, i.e. Ca, Sr and Ba, absorb the visible light with wavelength of $\lambda > 410$ nm due to color centers, although their photocatalytic activity may be weak. The accepter-doped perovskite-type oxides, known as a p-type semiconductor, exhibit proton (H^+) conduction at high temperatures as 873 K [13–15]. Water vapor dissolves as proton (H^+) into the oxides via holes (h^+) and oxygen vacancies. Thus, we may expect that, at room temperature, this type of oxides may adsorb ions participating in photocatalytic reactions. One objective of the present work is to examine whether the composite powders having the junctions of n-type TiO_2 with the p-type oxides exert higher photocatalytic activity than sole TiO_2 particles under the irradiation of Xe discharge light. Another objective is to examine whether the photocatalytic activity for the visible light can be produced by the composite.

2. Experimental

2.1. Materials

As the p-type semiconducting oxide absorbing visible light, we used the perovskite-type $SrZrO_3$ oxide doped with 5 and 10 mol% $YO_{3/2}$, i.e. $Sr(Zr_{0.90}Y_{0.05})O_{3-\delta}$ and

---

* Corresponding author. Tel.: +81-6-6879-7461; fax: +81-6-6879-7461.
E-mail address: shinya@mat.eng.osaka-u.ac.jp (S. Otsuka-Yao-Matsuo).

1010-6030/03/$ – see front matter © 2003 Elsevier Science B.V. All rights reserved.
PII: S1010-6030(02)00405-7

$Sr(Zr_{0.90}Y_{0.10})O_{3-\delta}$ and the perovskite-type $CaZrO_3$ oxide doped with 10 mol% $YO_{3/2}$ and 5 mol% $GaO_{3/2}$, i.e. $Ca(Zr_{0.95}Y_{0.10})O_{3-\delta}$ and $Ca(Zr_{0.90}Ga_{0.05})O_{3-\delta}$. Powdered raw materials $SrCO_3$ (3N), $CaCO_3$ (3N), ZrO_2 (HfO_2: 1.2 mass%, Fe: 0.001 mass%, P <0.003 mass%, Na_2O <0.002 mass%, Cl <0.01 mass%), Y_2O_3 (3N) and Ga_2O_3 (4N) were weighed and thoroughly mixed using a zirconia mortar, and then fired at 1723 K for 10 h. After the grinded powders were pressed into a 9-mm-diameter disk under 265 MPa and loaded in Pt crucible, it was annealed at 1923 K for 50 h. The disk was crushed and pulverized using the zirconia mortar. It was judged from the change in the lattice constant that the doping elements substituted at the Zr ion site of the perovskite-type oxides. As the n-type semiconductor, we used the anatase-type TiO_2 powder commercialized (Ishihara Sangyo, ST-01).

The composite powders involving the pn-junction were prepared in a simple manner. After the TiO_2 and perovskite-type oxide powders were mixed in mass ratios of $(100-z):z$, they are fired at 973 K for 1 h without pelletizing, and then milled lightly for 5 min using the zirconia mortar.

2.2. Evaluation of the photocatalytic activity

The photocatalytic activity of the sample powders was evaluated by the photodegradation of methylene blue [16] and formic acid (HCOOH) [8] aqueous solutions. The 2×10^{-5} M methylene blue aqueous solution (100 ml) with the sample powders (0.20 g) was loaded in a glass container (30 cm^2) and stirred with a magnetic stirrer under the irradiation of 500 W Xe discharge light above it. After the 12 ml of the solution was sucked and subjected to centrifugation, the optical absorption spectra for the supernatant solution was recorded by the double beam spectrophotometer (Hitachi U4000).

It was reported that the photocatalytic oxidations of HCOOH proceeds according to the total reaction [8],

$$\mathrm{HCOOH\ (aq.)} + \tfrac{1}{2}\mathrm{O_2\ (gas)} \rightarrow \mathrm{CO_2\ (gas)} + \mathrm{H_2O\ (liq.)}.$$

The decomposition of 1 mol of HCOOH leads to the evolution of 1/2 mol gases. The 0.02 M HCOOH aqueous solution (100 ml) with the sample powders (0.20 g) was loaded in a glass container (45 cm^2) kept at 303 K and stirred with a magnetic stirrer under the irradiation of 500 W Xe discharge light above it. The increase in the volume of the gas phase was measured using the Sievert's apparatus as shown in Fig. 1.

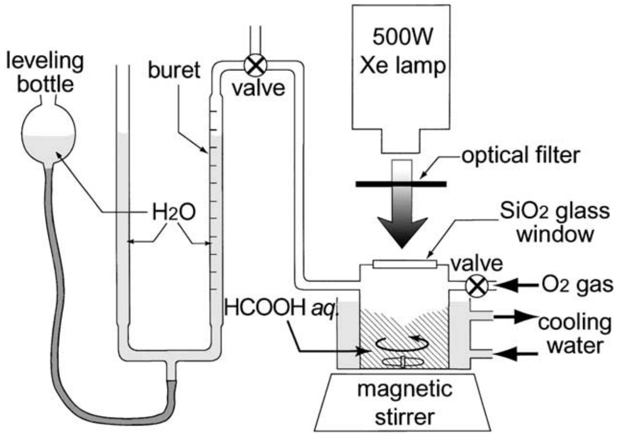

Fig. 1. Sievert's apparatus used for detection of the evolved gases by HCOOH decomposition.

3. Experimental results and discussions

The accepter-doped perovskite oxide powders prepared by the conventional ceramic method were grayish blue or pink, and absorbed the light with wavelength of $\lambda < 800$ nm due to its fundamental absorption and colorations induced by defects. As the coloration depended on the atmosphere for the annealing, the defects related to oxygen, e.g. oxygen vacancies such as $V_O^{\bullet\bullet}$, $V_O^{\bullet}$ and $V_O^{\times}$ and oxygen at interstitial sites, such as O_i', O_i'' and $O_i^{\times}$, may be considered as color centers. Figs. 2 and 3, respectively, show the X-ray diffraction patterns and diffuse reflectance spectra of the perovskite-type Y_2O_3-doped Sr–Zr–O oxides. The diffraction peak due to $SrCO_3$ was very small and did not depend on the amount of Y_2O_3 doped. Further, with the addition of Y_2O_3, the diffraction peaks due to the oxides slightly shifted toward smaller diffraction angle. Similar results were obtained for Y_2O_3-doped Ca–Zr–O and Ga_2O_3-doped Ca–Zr–O oxides. Thus, it was found that the Y and Ga ions substituted at the Zr ion sites of $SrZrO_3$ and $CaZrO_3$, i.e. B sites of the ABO_3 perovskites. Fig. 4 shows the X-ray diffraction patterns of the TiO_2 (ST-01) and the composite powders, respectively, fired at 973 K for 1 h in air. The TiO_2 was composed of the anatase-type phase as purchased, and the rutile-type phase was not detected.

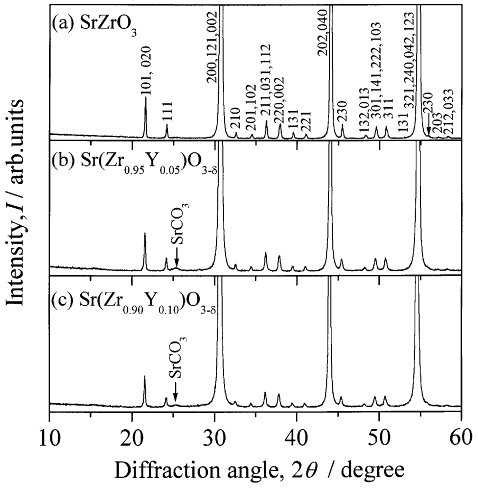

Fig. 2. X-ray diffraction patterns for perovskite type $Sr(Zr_{1-x}Y_x)O_{3-\delta}$ prepared.

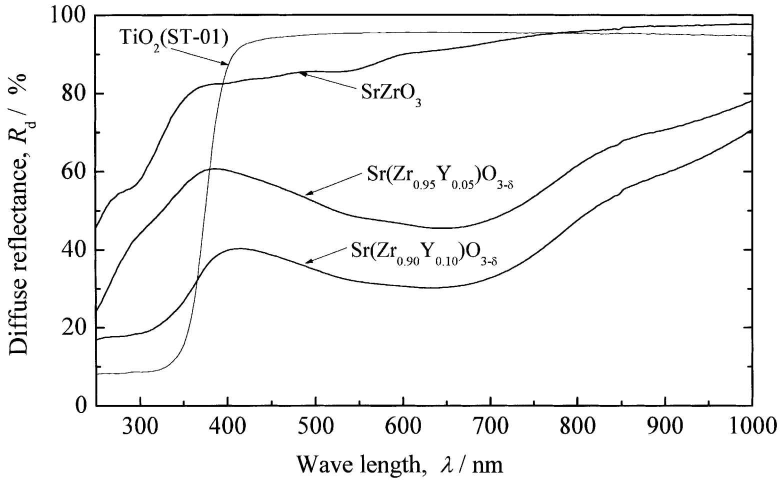

Fig. 3. Diffuse reflectance spectra of perovskite type $Sr(Zr_{1-x}Y_x)O_{3-\delta}$ compared with those of TiO_2 and $SrZrO_3$.

Figs. 5(a) and 5(b) show variation in the absorption spectrum of methylene blue aqueous solution under the irradiation of Xe discharge light, when the composite powders of TiO_2 and $Sr(Zr_{0.90}Y_{0.10})O_{3-\delta}$ and the sole TiO_2, respectively, were used as photocatalyst. In the both cases, the characteristic absorption peak of the methylene blue around 664 nm was decreased and slightly shifted toward a shorter wavelength, and finally the solution became colorless. The ST-01 commercialized powder of anatase-type TiO_2 is known as having a relatively high photocatalytic activity. When the composite powders of TiO_2 and $Sr(Zr_{0.90}Y_{0.10})O_{3-\delta}$ oxides were used as a sample, the photobleaching of methylene blue proceeded faster than a sole TiO_2. In Fig. 6, variations in the maximum absorbance in the wavelength ranging between 600 and 664 nm with time are compared for various composite powders involving $z = 10$ mass% of perovskite powder. The preliminary treatment, i.e. drying at 413 K and firing at 973 K, did not have significant effect on the results for a sole TiO_2 powder; this result is consistent with the XRD analysis, i.e. the starting anatase-type TiO_2 phase did not transform to the rutile-type phase upon heating up to 973 K. When a sole $Sr(Zr_{0.90}Y_{0.10})O_{3-\delta}$ powder was used, the photobleaching rate was approximately equivalent with that without the sample (blank test). A sole $Sr(Zr_{0.90}Y_{0.10})O_{3-\delta}$ powder appeared to have no effect on the photodegradation of the methylene blue; the photocatalytic activity of the perovskite-type zirconate appeared to be very weak. Surprisingly, when the composite powder of TiO_2 and $Sr(Zr_{0.90}M_{0.10})O_{3-\delta}$ oxides were used as a sample, the photobleaching proceeds several times faster than TiO_2. Before the irradiation, the composite powders were white because of small amount of perovskite-type oxide contained. As the photobleaching proceeded, the sample powder was colored in dark blue, and then turns back to the original white as the bleaching was completed. Similar results were obtained for composite powders of TiO_2 with the other perovskite-type zirconates. The coloring of the sample powders indicates the strong adsorption of the methylene blue ions on the sample. The particle size of the perovskite powders prepared in this study was large as 10 μm, while the starting size of the ST-01 TiO_2 powder was smaller than 0.1 μm. According to SEM and TEM observation, the perovskite powder was surrounded by the TiO_2 fine powders aggregated, and any other compounds were not observed. When the perovskite-type powders were left in air at room temperature as long as 1 month, the self-pulverization occurred probably due to the water vapor in air. The particle became small so that we could not observe the junction between the perovskite-type and TiO_2 particles in the composite powders. For the self-pulverized composite powders, the photobleaching rate of the methylene blue became fastest as shown in Fig. 6.

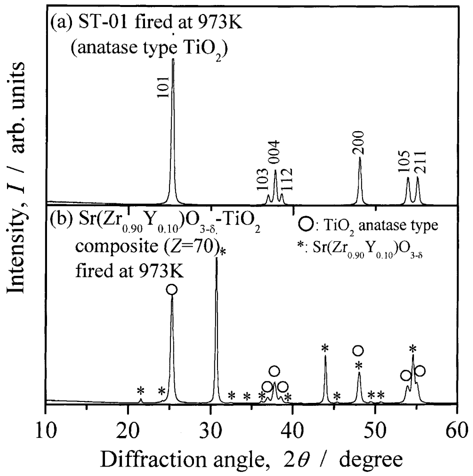

Fig. 4. X-ray diffraction patterns for TiO_2 and composite powders fired at 973 K: (a) TiO_2 powder, (b) $Sr(Zr_{0.90}Y_{0.10})O_{3-\delta}$-$TiO_2$ composite powder($z = 70$ mass%). All the diffractions for TiO_2 could be indexed as those for anatase-type structure. (○) Anatase-type TiO_2; (∗) perovskite-type Sr $(Zr_{0.90}Y_{0.10})O_{3-\delta}$.

Fig. 7 shows the dependence of the bleaching rate on the mass%, z, of the perovskite in the composite powder

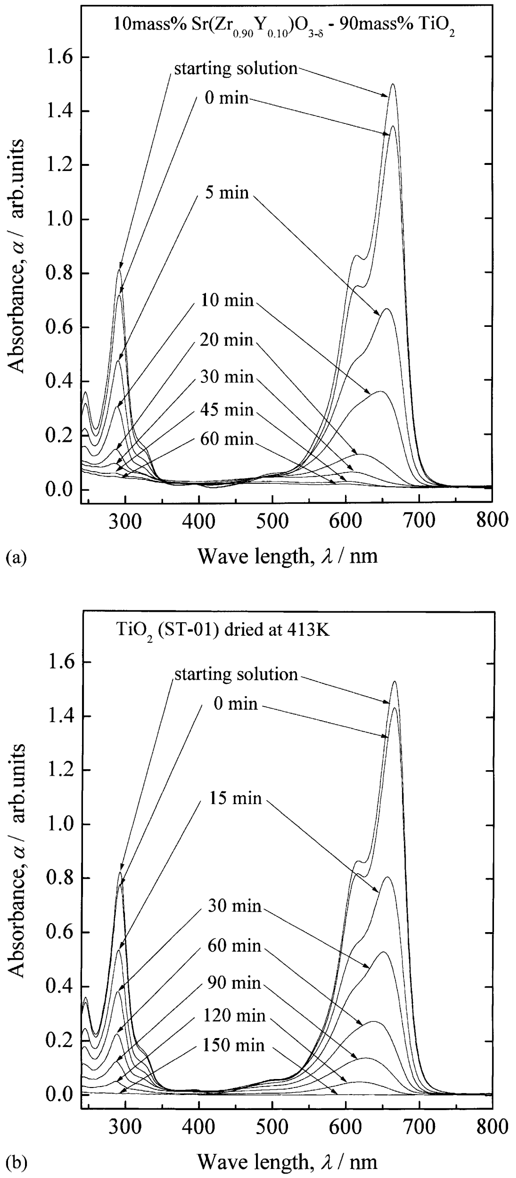

Fig. 5. Variation in the absorption spectrum of methylene blue aqueous solution under unfiltered irradiation of 500 W Xe lamp. The concentration of methylene blue for the starting solution was 2.0×10^{-5} mol dm^{-3}. (a) Sensitized by the Sr(Zr$_{0.90}$Y$_{0.10}$)O$_{3-\delta}$-TiO$_2$ composite powders ($z = 10$ mass%) possessing pn-junction, (b) TiO$_2$ powder dried at 413 K.

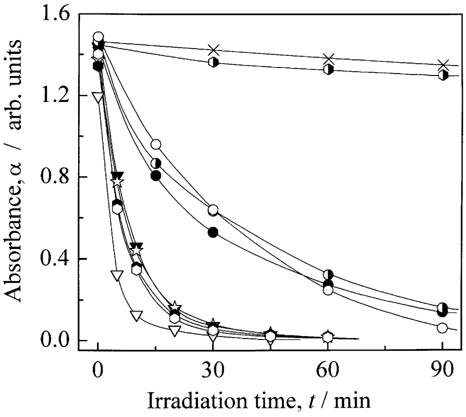

Fig. 6. Change in the maximum absorbance in the wavelength range of 600 and 664 nm of methylene blue under unfiltered irradiation of 500 W Xe discharge light. The amount of the perovskite-type oxides in the composites with TiO$_2$ is $z = 10$ mass%. (×) Without sample powders (blank test); (●) TiO$_2$ dried at 413 K ($\Delta_{\mathrm{abs}} = 0.054\,\mathrm{min}^{-1}$); (○) TiO$_2$ fired at 973 K; (◑) TiO$_2$ as received; (◑) Sr(Zr$_{0.90}$Y$_{0.10}$)O$_{3-\delta}$ powder; (●) Sr(Zr$_{0.90}$Y$_{0.10}$)O$_{3-\delta}$-TiO$_2$ composite ($\Delta_{\mathrm{abs}} = 0.205\,\mathrm{min}^{-1}$); (○) Sr(Zr$_{0.95}Y_{0.05}$)O$_{3-\delta}$-TiO$_2$ composite; (▼) Ca(Zr$_{0.90}$Y$_{0.10}$)O$_{3-\delta}$-TiO$_2$ composite; (▽) Ca(Zr$_{0.90}$Y$_{0.10}$)O$_{3-\delta}$-TiO$_2$ composite left in air at room temperature for more than 1 month; (☆) Ca(Zr$_{0.95}$Ga$_{0.05}$)O$_{3-\delta}$-TiO$_2$ composite.

of TiO$_2$ and Sr(Zr$_{0.90}$Y$_{0.10}$)O$_{3-\delta}$ oxides. The bleaching rate appeared to be maximum around z = 20–40 mass%; the result may correspond to change in the area of the pn-junction. Fig. 8 shows the variation of absorbance with time under the condition of visible light irradiation with $\lambda > 420$ nm using L42 sharp-cut filter. For TiO$_2$ ($z = 0$) and Sr(Zr$_{0.90}$Y$_{0.10}$)O$_{3-\delta}$ rich powder ($z = 90$), the photocatalytic degradation was not observed, while a clear degradation was observed for $z = 50$. These results indicate that photoexcited electrons and holes were generated in the perovskite by the visible light, and then, plausibly the electron flowed through the pn-junction into TiO$_2$. Thus, we could infer that the area of the pn-junction, amount of the perovskite and the micro-distribution of the two phases become important factor for the catalytic activity under visible light irradiation.

Fig. 9 shows the results on the photocatalytic degradation of HCOOH aqueous solution. When the TiO$_2$ was used as the catalyst, the gas volume was smoothly increased due to the CO$_2$ gas evolved and reached to a constant value in 100 min under unfiltered light irradiation. The volume of the gas

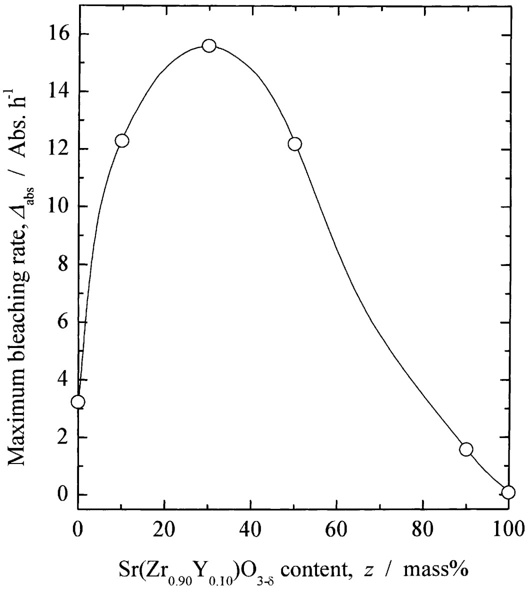

Fig. 7. Dependence of the maximum rate of decrease in the absorbance Δ_{abs}, on the mass percent z, of Sr(Zr$_{0.90}$Y$_{0.10}$)O$_{3-\delta}$ in the composites with TiO$_2$, under the unfiltered irradiation of 500 W Xe discharged light.

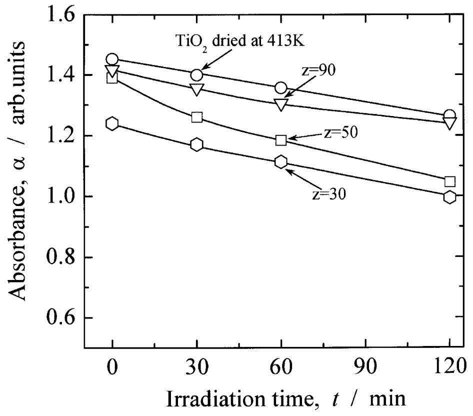

Fig. 8. Change in the maximum absorbance in the wavelength ranging between 600 and 664 nm of methylene blue under irradiation of visible light with $\lambda > 420$ nm using UV-cut filter (L42, Suruga Seiki Co. Ltd.). (○) TiO_2 powder dried at 413 K; (▽) $Sr(Zr_{0.90}Y_{0.10})O_{3-\delta}$-$TiO_2$ composite ($z = 90$ mass%); (□) $Sr(Zr_{0.90}Y_{0.10})O_{3-\delta}$-$TiO_2$ composite ($z = 50$ mass%); (⬡) $Sr(Zr_{0.90}Y_{0.10})O_{3-\delta}$-$TiO_2$ composite ($z = 30$ mass%).

evolved, i.e. the difference between the measured and blank values, was estimated as 0.7×10^{-3} mol. This is in satisfactory agreement with the calculated value of 1×10^{-3} mol, when considering the dissolution of the evolved CO_2 gas into the aqueous solution. Once the UV-cut filter, L42, was inserted in the light path, any increase in the gas volume was not observed, and rather the volume decreased very slowly due to a small leakage of apparatus system. When the composite of TiO_2 and 30 mass% $Sr(Zr_{0.90}Y_{0.10})O_{3-\delta}$ powder was used, the photodegradation rate of HCOOH under unfiltered light irradiation was approximately equivalent with that of a sole TiO_2. One may notice that the amount of TiO_2 in the composite is smaller than that for a sole TiO_2. Further, as seen in Fig. 9, even when the UV-cut filter, L42 was inserted in the light path, the photodegradation of HCOOH proceeded. This result is consistent with that for the photodegradation of the methylene blue; the composite of TiO_2 and $Sr(Zr_{0.90}Y_{0.10})O_{3-\delta}$ powders acted as a photocatalyst under visible light irradiation.

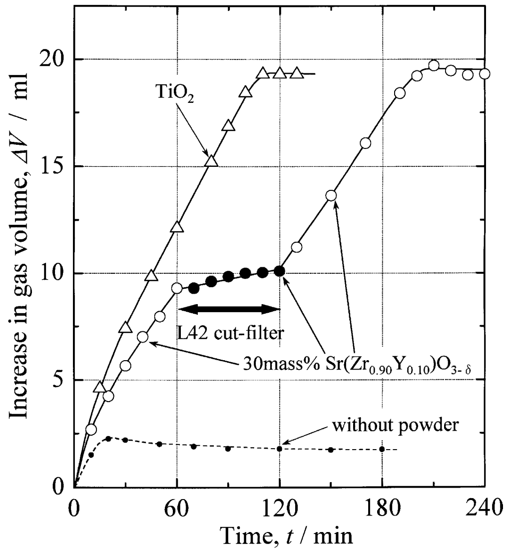

Fig. 9. Increase in gas volume as a function of time during the photocatalytic degradation of HCOOH aqueous solution. (△) TiO_2 powder under unfiltered irradiation of Xe discharge light, and (○ and ●) $Sr(Zr_{0.90}Y_{0.10})O_{3-\delta}$-$TiO_2$ composite ($z = 30$ mass%) under unfiltered irradiation of Xe discharge light and under irradiation of visible light with $\lambda > 420$ nm using UV-cut filter, respectively.

The higher photocatalytic activity of the composite than the sole TiO_2 may be attributable to a success in the spatial separation of the electrons and holes photogenerated in the composite particles. When the firing temperature for the composite preparation was between 873 and 973 K, we obtained similar results for the photocatalytic activity. The rutile-type TiO_2 phase was not detected in these composites. The photocatalytic activity of the composite powder prepared by a strong milling was smaller than that prepared by a moderate milling. Thus, the authors have inferred that the composite effect came from the flow of the photogenerated charges through the pn-junctions in the composite particles. Although the electronic band structure of the acceptor-doped perovskite-type oxides, especially involving oxygen-related defects, is not clear, a plausible situation for the particles having an equivalent size may be schematically shown in Fig. 10. In the p- and n-types semiconductors dipped into aqueous solutions, the conduction and valence bands, respectively, exhibit a down-hill curve toward the surface of the particle for the p-type and a up-hill curve toward the surface for the n-type [17]. The electronic structure near the energy band gap, along the X_1–X_2 line, is illustrated in a generalized form of pn-junction in Fig. 10(b). When the energy band gap for the p-type is smaller than that for the n-type TiO_2, more electrons are formed in the p-type. They diffuse on the surface of the p-type near the pn-junction, because the electrons diffuse toward the n-type through the junction. As the photogenerated electrons gather on the surface of the p-type, the adsorbed substances with positive charges are piled up and then gradually fall down toward the n-type. Thus, the electrons photogenerated in the n-type TiO_2 are attracted toward the surface near the pn-junction. The photogenerated holes in it move toward the surface far from the junction. Some of them excited near pn-junction may diffuse through the junction toward the surface of the p-type far from the junction, where the holes photogenerated in the p-type also gather. Although the electrons and holes move in opposite direction through the pn-junction, their recombination may be scarce. The electrons and holes, respectively, may diffuse near the surface and center due to the adsorbed substances with positive charge.

Strictly speaking, the pn-junction in the composite is just a model to explain the present experimental results. One may infer some catalytic effect of the perovskite phase. However, as described earlier, each perovskite particle was surrounded by the TiO_2 fine powders aggregated, especially for the TiO_2-rich composition. The spatial separation of the photogenerated charges is of great important to proceed

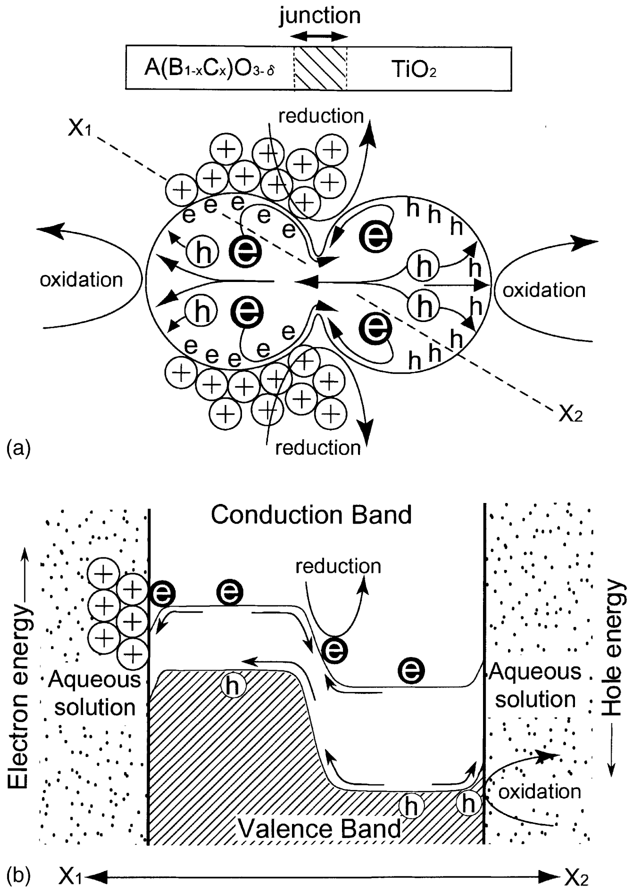

Fig. 10. Plausible drawing of the flows and spatial separations of the photogenerated electrons and holes in a composite particle possessing pn-junction: (a) in 2D, and (b) electronic structures along the X_1–X_2 cross-sectional line.

the photocatalytic reaction efficiently; the charges separation promotes the adsorption of ionized substances to be degraded. Such a separation appears to be induced by the charges flow through the pn-junction in the composite of TiO_2 with the acceptor-doped perovskite-type oxides. Although the perovskite-type oxides used in this study did not have a photocatalytic activity, they enhanced the activity of the composite with TiO_2. Furthermore, the perovskite oxides induced the photocatalytic activity for visible light; this result may imply the photo-excitation of charges via defect levels in the perovskite-type oxides. The phenomena observed in this study may become useful for design of the photocatalytic semiconductors acting under visible light.

4. Conclusions

The photocatalytic activity of the composite particles has been examined for the photodegradation of methylene blue and HCOOH aqueous solutions. The composite powders were prepared by mixing the titanium dioxide and acceptor-doped perovskite-type oxides involving SrO and CaO.

(1) Although the photocatalytic activity of the perovskite-type oxide $Sr(Zr_{0.90}Y_{0.10})O_{3-\delta}$ is weak, it absorbs light with wavelength of $\lambda < 800$ nm.
(2) Under the irradiation of unfiltered Xe discharged light, the composite particles exerted several times higher photocatalytic activity in photodegradation of methylene blue than a sole TiO_2. Similar results were obtained for the composite powders of $Sr(Zr_{0.95}Y_{0.05})O_{3-\delta}$, $Ca(Zr_{0.95}Y_{0.10})O_{3-\delta}$ and $Ca(Zr_{0.95}Ga_{0.05})O_{3-\delta}$ with TiO_2, respectively.
(3) Under the irradiation of the visible light with wavelength of $\lambda > 420$ nm, when the composite powder of TiO_2 and $Sr(Zr_{0.90}Y_{0.10})O_{3-\delta}$ was used, the photodegradation of methylene blue and HCOOH aqueous solutions proceeded.
(4) These results may be explained by a model for the flow of the photogenerated electrons and holes through the pn-junctions in the composite particles; the charges flow through the pn-junctions leads to their spatial separation. The phenomena observed in this work may be useful for design of photocatalytic semiconductors acting for visible light.

Acknowledgements

The authors would like to express thank to Mr. Kita for his experimental assistance.

References

[1] A. Fujishima, K. Honda, Bull. Chem. Soc. Jpn. 44 (1971) 1148.
[2] A. Fujishima, K. Honda, Nature 238 (1972) 37.
[3] A. Fujishima, T.N. Rao, A. Tryk, J. Photochem. Photobiol. Part C: Photochem. 1 (2000) 1.
[4] K. Domen, J.N. Kondo, M. Hara, T. Takata, Bull. Chem. Soc. Jpn. 73 (2000) 1307.
[5] A. Kudo, J. Ceram. Soc. Jpn. 109 (2001) S81.
[6] A.J. Nozik, Appl. Phys. Lett. 30 (1977) 567.
[7] K. Tennakone, J. Bandara, Sol. Energy Mater. Sol. Cells 60 (2000) 361.
[8] A. Hattori, Y. Tokihisa, H. Tada, S. Ito, J. Electrochem. Soc. 147 (2000) 2279.
[9] Y. Zhang, L. Shi, Z. Zhang, J. Shanghai University (Natural Sci.) 6 (2000) 333.
[10] T.-K. Young, Y.-S. Kang, I.-L. Wan, J.-C. Guang, R.-D. Young, J. Catal. 191 (2000) 192.
[11] T. Watanabe, K. Hashimoto, Kurin Tekunoroji 11 (2001) 30.
[12] T. Tatsuma, S. Saitoh, Y. Ohko, A. Fujishima, Chem. Mater. 13 (2001) 2838.
[13] H. Iwahara, T. Esaka, H. Uchida, N. Maeda, Solid State Ion. 3/4 (1981) 359.
[14] T. Yajima, H. Kazeoka, T. Yogo, H. Iwahara, Solid State Ion. 47 (1991) 271.
[15] T. Omata, S. Otsuka-Yao-Matsuo, J. Electrochem. Soc. 148 (2001) E252.
[16] A. Mills, J. Wang, J. Photochem. Photobiol. Part A: Chem. 127 (1999) 123.
[17] R. Memming, Electrochim. Acta 25 (1980) 77.